

# Detecting Individual Electrons Using a Carbon Nanotube Field-Effect Transistor

Andreas Gruneis, Maria J. Esplandiu, Daniel Garcia-Sanchez, and  
Adrian Bachtold\*

*CIN2 Barcelona and CNM-CSIC, Campus UAB, E-08193 Bellaterra, Spain*

*Received September 4, 2007; Revised Manuscript Received October 24, 2007*

## ABSTRACT

We study a simple highly resistive molecular circuit by detecting the transfer of individual electrons. The circuit consists of a Au nanoparticle, a carbon nanotube transistor, and a gate electrode, and the tube–particle resistance is about  $10^{19} \Omega$ . The high-impedance measurements are carried out by counting the electrons that are transferred onto the particle using the nanotube transistor as the charge detector. These measurements allow for the electron characterization of the circuit. In addition, single-electron detection is used to determine the separation between the electron states in the particle or to monitor the decay in time of the electron number in the particle.

The detection and manipulation of individual electron charges are among the ultimate goals of nanoscale electronics. It holds promise for ultralow dissipative circuits as well as for information processing in highly resistive molecular circuits. Carbon nanotube field-effect transistors<sup>1,2</sup> offer unique opportunities for single-electron detection. Nanotubes have ultrasmall cross sections, and their conducting electrons are located at the tube surface. These advantages have been exploited for the sensing of chemical gas<sup>3,4</sup> and biological probes.<sup>5,6</sup> Nanotubes have also been used to detect packets of multiple electrons transferred from the nanotube onto a particle, though the precise number of electrons in the packet could not be measured.<sup>7</sup> Single-electron detection has been resolved for electrons hopping onto defects randomly trapped in the substrate.<sup>8–12</sup> However, these single-electron processes remain poorly controlled. Different defects can be probed in parallel, so the electron properties of the circuit can be only partially characterized.

In this letter, we demonstrate for the first time single-electron detection on a nanosystem that is not a defect,<sup>8–12</sup> namely, a gold nanoparticle. This well-defined circuit allows for the full electron characterization of the circuit (Figure 1b) using single-electron detection measurements. We determine the different capacitances in the circuit, the separation between the electron states in the particle, and the tunnel resistance between the particle and the nanotube. The resistance is about  $10^{19} \Omega$  and corresponds to a transfer rate as low as  $\sim 0.001 \text{ s}^{-1}$ . Such a low transfer rate, together with the well-defined circuit, allows us to inject and extract different electrons from the particle under out-of-equilibrium conditions and to monitor the electron number decay in time.

Carbon nanotube transistors are fabricated by means of standard nanofabrication techniques. Tubes are grown by chemical vapor deposition<sup>13</sup> on a doped Si wafer with a  $1 \mu\text{m}$  thermal silicon oxide layer. They are electrically contacted to Cr/Au electrodes patterned by electron-beam lithography. Gold nanoparticles are deposited onto the wafer from a suspension in water that consists of gold chloride and trisodium citrate. An  $\sim 30 \text{ nm}$  diameter particle is positioned on top of the tube by atomic force microscopy manipulation (Figure 1a,b).

The transfer of electrons onto the particle can be detected by measuring the conductance  $G_{\text{tube}}$  of the nanotube while sweeping the gate voltage  $V_G$  (Figure 2a) because the tube conductance is extremely sensitive to the presence of electric charges. As  $V_G$  is swept from  $-4$  to  $-1 \text{ V}$ , the conductance is turned off as for typical p-doped semiconducting SWNTs.<sup>1,2</sup> Moreover, we have observed 35 abrupt conductance jumps (vertical red bars) that indicate discrete electron transfer from the nanotube into the particle. Each extra electron in the particle changes the electrostatic potential in the particle and, in turn, the charge density  $\rho_{\text{tube}}$  in the nanotube, which shifts the conductance  $G_{\text{tube}}$  horizontally in  $V_G$ . Note that the electron-transfer events do not occur at periodic values of  $V_G$ , as shown in the inset of Figure 2a.

As the measurement is repeated, conductance jumps appear at different gate voltages (Figure 2b). This indicates the stochastic nature of the electron transfer, as illustrated in the inset of Figure 2b; see also below. Remarkably, repeated measurements fall on curves that are periodically spaced in gate voltage with a period of about  $\Delta V_G^{\text{shift}} = 60 \text{ mV}$ . The same spacing is observed over the  $V_G$  range spanning from the on- to the off-conductance (from  $-4$  to  $-1 \text{ V}$ ; see Figure 2a). This periodicity suggests that adjacent curves differ by

\* Corresponding author. E-mail: adrian.bachtold@cnm.es.

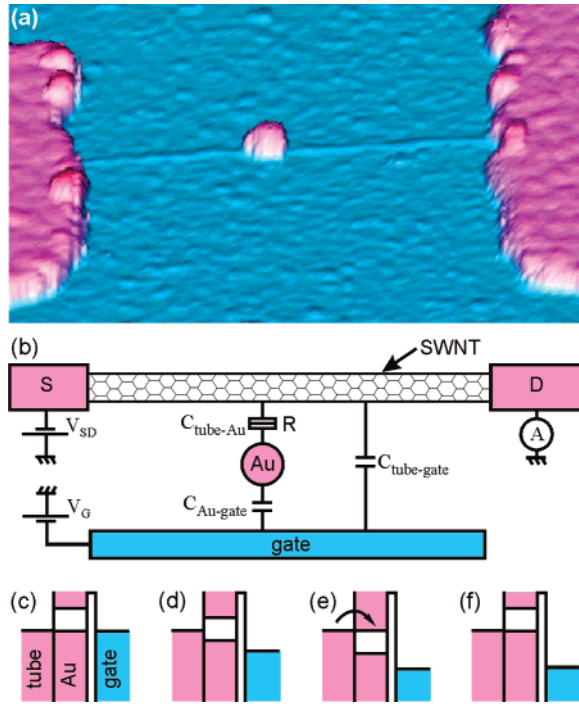


**Figure 1.** Device geometry. (a) Atomic force microscopy image of a Au nanoparticle placed on top of a SWNT, which is in contact with two metal electrodes. The separation between the metal electrodes is 600 nm. (b) Schematic of the measurement setup. The tube conductance is always measured with  $eV_{SD} < kT$ . (c–f) Schematics of the potentials in the nanotube and the particle as the gate potential is swept down. Each time an empty energy level of the particle matches the electrochemical potential of the tube, an electron is transferred onto the particle, which is detected by the nanotube transistor.

one electron in the Au particle and, in turn, that the observed jumps correspond to transfers of single electrons. Measurements on a second device yield a period of about 40 mV.

Measurements on devices without an Au particle look very different. Most often, no conductance jumps are observed at all. For some devices, jumps can be detected, but their number remains very low and no period in gate voltage can be assigned. Those jumps are attributed to uncontrolled charge traps at defects.

The mechanism that controls electron transfer onto the particle has a lot in common with what happens in a single-electron transistor.<sup>14,15</sup> Adding an electron to the particle costs the Coulomb charging energy  $E_C = e^2/(C_{\text{tube-Au}} + C_{\text{Au-gate}})$  (represented by a gap in Figure 1c). By reducing the gate potential  $E_G$  proportional to  $-eV_G$ , the potential of the Au particle  $E_{\text{Au}}$  decreases according to Kirchhoff's laws (Figure 1d). This is described by the first term in

$$E_{\text{Au}} = \frac{C_{\text{Au-gate}} E_G}{(C_{\text{Au-gate}} + C_{\text{tube-Au}})} + E_C N \quad (1)$$

When the tube's electrochemical potential matches the upper energy of the Coulomb gap in the particle (Figure 1e), an electron can be transferred from the tube onto the particle, and the electron number  $N$  in the particle is increased by 1.

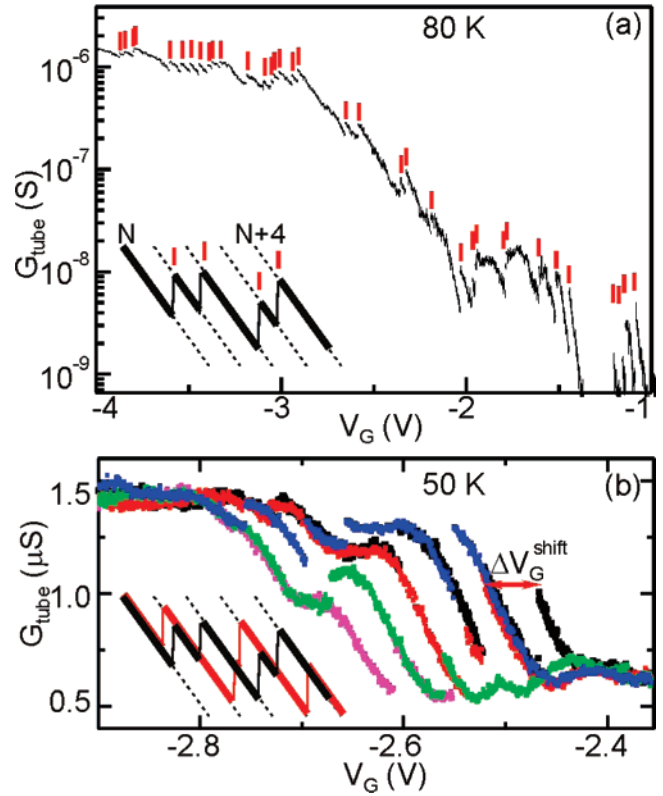


**Figure 2.** Detection of single electrons. (a) Tube conductance as the gate voltage  $V_G$  is swept from  $-4$  to  $-1$  V. Vertical red bars indicate conductance jumps. The recording time was 50 min. The inset shows the relation between  $G_{\text{tube}}(V_G)$  and the number of electrons in the Au particle. (b) Tube conductance as a function of  $V_G$ . Each color corresponds to a different scan. The sweep rate of  $V_G$  is the same for the different scans, 0.06 V/min. The magenta curve is shown for  $V_G$  between  $-2.9$  and  $-2.55$  V. The inset shows two traces of  $G_{\text{tube}}(V_G)$  in black and red; jumps appear at different  $V_G$  values as a result of the stochastic nature of the electron transfer.

This shifts  $E_{\text{Au}}$  by the amount  $E_C$  (Figure 1f), which blocks the transfer of the next electron. In contrast to previous single-electron transistors,<sup>15</sup> the transfer rate is slow enough to prevent the last electron from tunneling out of the particle by continuously sweeping down the gate potential.

We will now look at the time dependence of the electron transfers. For this purpose, the gate voltage is set at a fixed value while measuring the tube conductance (Figure 3). At 50 K, the tube conductance fluctuates between two values on a time scale of several hundred seconds. We attribute the two-level fluctuations to an electron going back and forth into the Au particle as a result of thermal excitation and thus changing the number of electrons between  $N$  and  $N + 1$ . As the temperature is increased to 150 K, the tube conductance fluctuates between three levels (i.e., between  $N$ ,  $N + 1$ , and  $N + 2$ ; Figure 3b). The mechanism is schematized in the insets of Figure 3.

The fluctuations of  $N$  due to thermal excitation provide information on the energy separation  $E_C$  between electron states of the Au particle. The two-level fluctuations at 50 K suggest that  $E_C$  is about  $kT$  (i.e.  $\approx 4$  meV; see inset of Figure 3a). Taking  $E_C \approx 50$  K gives  $C_{\text{tube-Au}} + C_{\text{Au-gate}} \approx 38$  aF, which is reasonable when considering that the self-

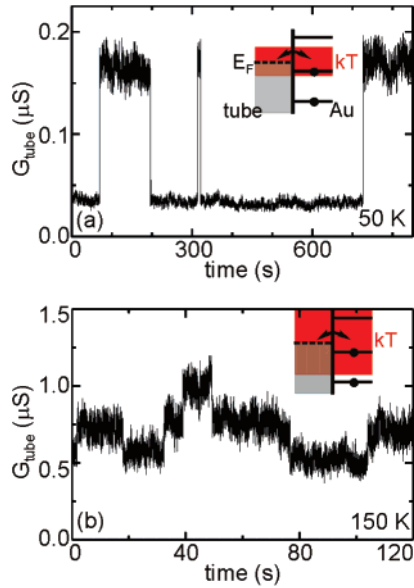


**Figure 3.** Fluctuations of the electron number due to thermal excitation. (a) Tube conductance as a function of time at 50 K for  $V_G = -1.35$  V. (b) Tube conductance as a function of time at 150 K for  $V_G = -1.2$  V. The conductance experiences two levels at 50 K and three levels at 150 K. Note that an extra level can appear at other  $V_G$  values. We attribute the extra level at 50 K to the electrochemical potential of the tube that matches the center of the Coulomb gap. The number of observed levels is on average 2.01 at 50 K and 3.1 at 150 K. The insets show the energy levels in the tube and in the Au particle for different numbers  $N$  of electrons. The thermal energy is shown in red.

capacitance of a sphere  $4\pi\epsilon_r\epsilon_0 r_{\text{Au}} = 7$  aF with  $\epsilon_r = 4$  and  $r_{\text{Au}} = 15$  nm has the same order of magnitude.

We will now exploit the low rate of charge transfer in order to manipulate the number of electrons on the particle under out-of-equilibrium conditions. To do this, the gate voltage is rapidly swept to change the potential of the Au particle, which positions different empty (occupied) electron levels of the Au particle below (above) the Fermi energy (schematic of Figure 4a). The number of empty levels depends on the amplitude of the gate voltage sweep. Measuring the tube conductance versus time allows us to monitor the decay toward equilibrium of the electron system (Figure 4a). As discussed previously, each conductance jump corresponds to the transfer of one electron.

The transfer rate changes as the temperature varies (Figure 4b). The average time for the three jumps in Figure 4a is shown to increase dramatically as the temperature  $T$  is reduced. This may be attributed to the shape of the tunnel barrier between the particle and the tube, for which the transmission is energy-dependent. Alternatively, this may be attributed to the transferred electrons that interact with phonons or other electrons. Additional studies need to be carried out to clarify this issue.

The above measurements allow us to estimate the tunnel resistance  $R$  between the particle and the tube. The average jump time  $\tau$  is given by  $e^2 R(1 - \exp(-\Delta E/kT))/\Delta E$  with  $\Delta E$  the energy difference between the tube and the particle.<sup>16</sup> For the case  $\Delta E \approx kT \approx E_C$

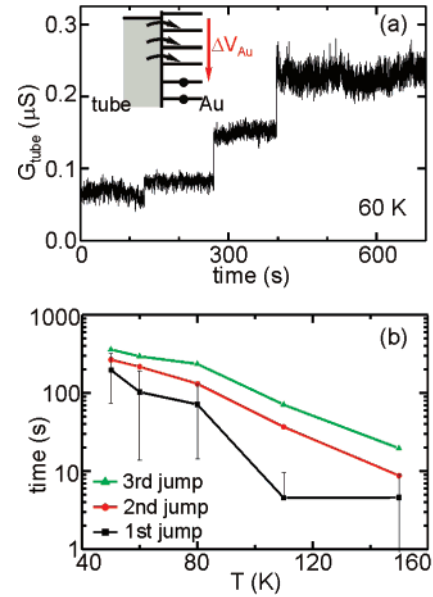


**Figure 4.** Manipulation of single electrons. (a) Tube conductance as a function of time after having rapidly increased the gate voltage by 0.4 V from  $-1.6$  to  $-1.2$  V. This results in the reduction of the potential in the particle as shown in the inset. The energy levels in the particle correspond to different numbers  $N$  of electrons. Note that the conductance height differs for the three jumps, which is attributed to the variation of the slope of  $G_{\text{tube}}(V_G)$ . (b) Average time of the first, second, and third jumps as a function of temperature. The standard error is shown for the first jump.

$$\tau \approx RC_{\text{tube-Au}} \quad (2)$$

Because  $C_{\text{tube-Au}} \approx e^2/E_C$ , we get  $R \approx 10^{19} \Omega$  at 50 K when  $\tau \approx 200$  s. Such a resistance is 6 orders of magnitude higher than what conventional electronics can cover. The resistance may originate from a gap of a few nanometers between the tube and the particle or from adsorbate layers at the tube–particle interface. This tunnel resistance could not be measured in previous single-electron detection experiments with nanotubes.<sup>7–12</sup>

The device can be further characterized by considering the electric circuit in Figure 1b. This circuit has been analyzed for silicon single-electron memory using a small floating gate, which represents the ultimate miniaturization of flash memory.<sup>8,17</sup> In this model, the conductance jumps in Figure 2a are on average separated by  $\Delta V_G^{\text{jump}}$ , and the adjacent curves in Figure 2b are separated by  $\Delta V_G^{\text{shift}}$  with

$$\Delta V_G^{\text{jump}} = \frac{e}{C_{\text{Au-gate}}} \quad (3)$$

$$\Delta V_G^{\text{shift}} = \frac{eC_{\text{tube-Au}}/(C_{\text{tube-Au}} + C_{\text{Au-gate}})}{(C_{\text{tube-gate}} + C_{\text{tube-Au}}C_{\text{Au-gate}}/(C_{\text{tube-Au}} + C_{\text{Au-gate}}))} \quad (4)$$

By taking the mean value of  $\Delta V_G^{\text{jump}} = 85$  mV,  $\Delta V_G^{\text{shift}} = 60$  mV, and  $E_C \approx 4$  meV, we get  $C_{\text{Au-gate}} = 1.8$  aF,  $C_{\text{tube-Au}} \approx 30$  aF, and  $C_{\text{tube-gate}} \approx 1$  aF. These values are reasonable considering the device geometry. Indeed,  $C_{\text{Au-gate}}$  can be roughly estimated by half the capacitance between two concentric spheres, which is  $2\pi\epsilon_r\epsilon_0(1/r_{\text{Au}} - 1/h)^{-1} \approx 3$  aF

with  $h$  being the oxide thickness.  $C_{\text{tube-gate}}$  is expected to be slightly less than half the capacitance between two coaxial cylinders, which is  $\pi\epsilon_r\epsilon_0 L/\ln(h/r_{\text{tube}}) \approx 9$  aF with  $L$  being the tube length.

The capacitance  $C_{\text{Au-gate}}$  quantifies the coupling between the Au particle and the gate.  $C_{\text{Au-gate}}$ , which is 1.8 aF, is remarkably large when considering that the gate is 1  $\mu\text{m}$  away from the Au particle. Compared to previous experiments on Au particles directly contacted to metal electrodes, the same coupling can be achieved provided that the separation between the gate and the Au particle is reduced to 2–3 nm.<sup>18,19</sup> This is because most of the electric field in the latter case is screened by the metal electrodes. Overall, our device layout enables efficient coupling, which allows access to a broad range of energy levels by sweeping the gate voltage. This is especially interesting for future studies on organic and biological molecules because the large energy separation between the levels often has limited access to only one level.<sup>20,21</sup>

We will now compare our work to other existing single-electron detectors, which are devices microfabricated in metal or semiconducting material working at milliKelvin temperatures.<sup>22–26</sup> The operation temperature (up to 150 K) of nanotube detectors is much higher. In addition, nanotubes are suitable for electron detection on systems that are physically different from the detector itself, such as molecules or nanoparticles. In contrast, microfabricated single-electron detectors so far have probed only systems structured with the same semiconducting or metal material as the detector. Moreover, these detectors are much larger, which is impractical for addressing molecules.

In conclusion, single-electron detection with a nanotube has been employed to characterize the equivalent circuit of a simple highly resistive molecular circuit. In this circuit, a Au nanoparticle is connected to a nanotube with an ultrahigh tunnel resistance of about  $10^{19} \Omega$ . Remarkably, such a resistance is 6 orders of magnitude higher than what conventional electronics can cover. We have also shown how single-electron detection can be used to extract the separation in energy between the electron states of the particle. Single-electron counting with nanotubes offers great promise for future studies on organic molecules, biomolecules, and semiconducting particles, which most often are highly resistive. Interestingly, the electron states of those systems are expected to depend not only on the charging energy but also on the molecular levels. Single-electron photoelectric effects can also be investigated, for instance, in CdSe particles,<sup>27</sup> as well as charge transfer in biomolecules involved in photosynthesis and respiration activities.<sup>28</sup> This technique may also provide information on internal electron-transfer events that occur within complex molecular systems.

**Acknowledgment.** We thank P. Gambardella, J. Moser, B. Placais, S. Sapmaz, and P. Gorostiza for discussions. This research has been supported by an EURYI grant and EU-funded project CARDEQ (FP6-IST-021285-2).

## References

- (1) Tans, S. J.; Verschueren, A. R. M.; Dekker, C. *Nature* **1998**, *393*, 49–51.
- (2) Martel, R.; Schmidt, T.; Shea, H. R.; Hertel, T.; Avouris, Ph. *Appl. Phys. Lett.* **1998**, *73*, 2447–2449.
- (3) Kong, J.; Franklin, N. R.; Zhou, C.; Chapline, M. G.; Peng, S.; Cho, K.; Dai, H. *Science* **2000**, *287*, 622–625.
- (4) Collins, P. G.; Bradley, K.; Ishigami, M.; Zettl, A. *Science* **2000**, *287*, 1801–1804.
- (5) Besteman, K.; Lee, J.-O.; Wiertz, F. G. M.; Heering, H. A.; Dekker, C. *Nano Lett.* **2003**, *3*, 727–730.
- (6) Star, A.; Gabriel, J. C. P.; Bradley, K.; Gruner, G. *Nano Lett.* **2003**, *3*, 459–462.
- (7) Marty, L.; Bonnot, A. M.; Bonhomme, A.; Iaia, A.; Naud, C.; Andre, E.; Bouchiat, V. *Small* **2006**, *2*, 110–115.
- (8) Durkop, T.; Kim, B. M.; Fuhrer, M. S. *J. Phys.: Condens. Matter* **2004**, *16*, R553–R580.
- (9) Liu, F.; Bao, M.; Kim, H. J.; Wang, K. L.; Li, C.; Liu, X.; Zhou, C. *Appl. Phys. Lett.* **2005**, *86*, 163102.
- (10) Ishigami, M.; Chen, J. H.; Williams, E. D.; Tobias, D.; Chen, Y. F.; Fuhrer, M. S. *Appl. Phys. Lett.* **2006**, *88*, 203116.
- (11) Lin, Y.-M.; Appenzeller, J.; Knoch, J.; Chen, Z.; Avouris, Ph. *Nano Lett.* **2006**, *6*, 930–936.
- (12) Peng, H. B.; Hughes, M. E.; Golovchenko, J. A. *Appl. Phys. Lett.* **2006**, *89*, 243502.
- (13) Kong, J.; Soh, H. T.; Cassell, A. M.; Quate, C. F.; Dai, H. *Nature* **1998**, *395*, 878–881.
- (14) Fulton, T. A.; Dolan, G. J. *Phys. Rev. Lett.* **1987**, *59*, 109–112.
- (15) Sohn, L. L.; Kouwenhoven, L. P.; Schon, G. *Mesoscopic Electron Transport*; Kluwer: Dordrecht, The Netherlands, 1997.
- (16) Pekola, J. P.; Hirvi, K. P.; Kauppinen, J. P.; Paalanen, M. A. *Phys. Rev. Lett.* **1994**, *73*, 2903–2906.
- (17) Yano, K.; Ishii, T.; Sano, T.; Mine, T.; Murai, F.; Hashimoto, T.; Kobayashi, T.; Kure, T.; Seki, K. *Proc. IEEE* **1999**, *87*, 633–651.
- (18) Magnus, Persson, S. H.; Olofsson, L.; Gunnarsson, L. *Appl. Phys. Lett.* **1999**, *74*, 2546–2548.
- (19) Bolotin, K. I.; Kuemmeth, F.; Pasupathy, A. N.; Ralph, D. C. *Appl. Phys. Lett.* **2004**, *84*, 3154–3156.
- (20) Park, J.; Pasupathy, A. N.; Goldsmith, J. I.; Chang, C.; Yaish, Y.; Petta, J. R.; Rinkoski, M.; Sethna, J. P.; Abruna, H. D.; McEuen, P. L.; Ralph, D. C. *Nature* **2002**, *417*, 722–725.
- (21) Liang, W.; Shores, M. P.; Bockrath, M.; Long, J. R.; Park, H. *Nature* **2002**, *417*, 725–728.
- (22) Lu, W.; Ji, Z.; Pfeiffer, L.; West, K. W.; Rimberg, A. J. *Nature* **2003**, *423*, 422–425.
- (23) Elzerman, J. M.; Hanson, R.; Willems, van Beveren, L. H.; Witkamp, B.; Vandersypen, L. M. K.; Kouwenhoven, L. P. *Nature* **2004**, *430*, 431–434.
- (24) Bylander, J.; Duty, T.; Delsing, P. *Nature* **2005**, *434*, 361–364.
- (25) Gustavsson, S.; Leturcq, R.; Simovic, B.; Schleser, R.; Ihn, T.; Studerus, P.; Ensslin, K.; Driscoll, D. C.; Gossard, A. C. *Phys. Rev. Lett.* **2006**, *96*, 076605.
- (26) Fujisawa, T.; Hayashi, T.; Tomita, R.; Hirayama, Y. *Science* **2006**, *312*, 1634–1636.
- (27) Gudiksen, M. S.; Maher, K. N.; Ouyang, L.; Park, H. *Nano Lett.* **2005**, *5*, 2257–2259.
- (28) Gray, H. B.; Winkler, J. R. *Proc. Natl. Acad. Sci. U.S.A.* **2005**, *102*, 3534–3539.

NL072243W